

Stability of a Plane Parallel Flow with Variable Vertical Shear and Unstable Stratification

By Tomio Asai*

*National Center for Atmospheric Research**, Boulder, Colorado 80302, U.S.A.
(Manuscript received 13 November 1969)*

Abstract

A study is made of stability properties of perturbations superimposed on an unstably stratified plane parallel flow with variable vertical shear. Two different types of instability which may take place in the flow are found: one is a thermal instability modified by a shear flow, and the other is an inertial instability modified by a thermal stratification. Unstable perturbations of the thermal type are distinguished from those of the inertial type in terms of the Richardson number. The thermal instability is most favorable for development of a three-dimensional longitudinal perturbation whose wavelength in the direction parallel to the basic flow is much longer than that in the direction perpendicular to the basic flow. A preferred perturbation of the inertial instability, however, is of a two-dimensional transverse mode.

Amplification of transverse perturbations of thermal origin is reduced by the influence of a shear flow regardless of the presence of variable shear in the basic flow. We conclude that a shear flow in general is responsible for the formation of longitudinal convection roll, and a variable shear slightly affects characteristics of thermal instability of a constant shear flow.

1. Introduction

One of the cloud bands most frequently observed in the atmosphere is a system of long rows of cumulus clouds stretching in a general wind direction. Since Jeffrey's (1928) suggestion, a number of studies have been made both experimentally (Terada 1928, Graham 1934, Chandra 1938, etc.) and theoretically (Kuo 1963, Asai 1964 and 1970, Deardorff 1965, Gallagher and Mercer 1965, Ingersoll 1966, etc.) from the point of view of thermal convection in a shear flow. These studies concluded that a constant shear flow exerts a suppressing influence on convective motion in a vertical plane parallel to the basic flow in which the convection is imbedded and this is responsible for the formation of a longitudinal roll. This longitudinal roll forms a cloud band parallel to the general wind. On the other hand, Kuettner (1959 and 1967) suggested that the banded structure of clouds might be attributed to convection in heated air flows with a curved velocity profile

of rather uniform direction. Kuettner's conjecture was based on observations indicating that most cloud bands line up in the direction of flow whose characteristic wind profile in the vertical has a jet-like curvature.

According to the theory of hydrodynamic instability, a plane Couette flow is stable for small perturbations of any wavenumber (Riis 1962, Deardorff 1963, etc.), while a shear flow with a certain velocity profile may be unstable for small perturbations (Rayleigh 1880). Hence it is probable that the presence of a variable vertical shear flow in an unstably stratified fluid may affect thermal convection in the flow. The objective of this paper is to investigate the possible influence of variable vertical shear flow on a thermal convection based on a perturbation analysis.

2. Governing equations

Consider the flow of an unstably stratified fluid between two horizontal parallel planes. The velocity and the temperature of the flow which is parallel to the x axis are assumed to be functions of the height, z , only (Fig. 1). Perturbations of small amplitudes are superimposed on the flow.

We shall employ a system of linearized equations

* On leave from the Geophysical Institute, Kyoto University, Kyoto, Japan.

** The National Center for Atmospheric Research is sponsored by the National Science Foundation.

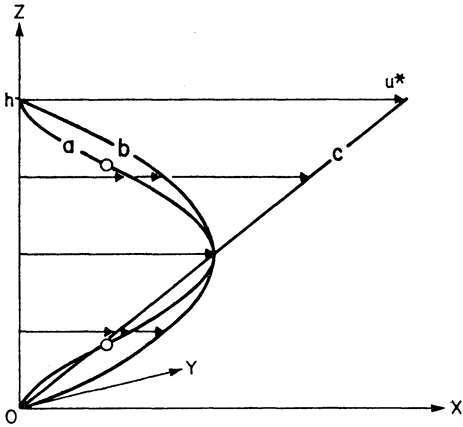


Fig. 1. The coordinate system and the profiles of the basic flow for three cases whose stability properties are studied: (a) a shear flow with points of inflection denoted by circles, (b) a plane Poiseuille flow, and (c) a plane Couette flow.

governing the perturbations in a stratified parallel shear flow under the Boussinesq approximation. The system of equations is also used by Asai (1970) in the study of thermal convection in a plane Couette flow. In order to express the linearized perturbation equations in dimensionless forms, the units of length $[L]$, time $[t]$, and temperature $[T]$ are defined as

$$\begin{aligned} [L] &= h \\ [t] &= h/u^* \\ [T] &= T^* \end{aligned}$$

where h is the depth of the fluid layer, u^* is a characteristic velocity of the basic flow as indicated in Fig. 1, and T^* is the imposed temperature difference between the upper and the lower boundary planes. The Reynolds number Re , the Rayleigh number Ra , the Richardson number Ri , and the Prandtl number Pr are defined as follows:

$$\begin{aligned} Re &= hu^*/\nu, & Ra &= g\alpha h^3 T^*/(\kappa\nu) \\ Ri &= g\alpha h T^*/u^{*2}, & Pr &= \nu/\kappa \end{aligned}$$

where ν is the coefficient of kinematic viscosity, κ is the coefficient of thermometric conductivity, α is the coefficient of thermal expansion, and g is the acceleration due to gravitational force. Note that a relationship, $Ra = Pr Ri Re^2$, exists among the four dimensionless parameters. Since we are concerned here with unstable stratification, the temperature at the lower boundary is higher than that at the upper boundary and Ri defined here

has a sign opposite from the conventional one.

Then the dimensionless perturbation equations for w' and T' are written as

$$\begin{aligned} \left(\frac{\partial}{\partial t} + \bar{u} \frac{\partial}{\partial x} - Re^{-1} \nabla^2 \right) \nabla^2 w' \\ - \frac{d^2 \bar{u}}{dz^2} \frac{\partial w'}{\partial x} - Ri \nabla^2 T' = 0 \end{aligned} \quad (2.1)$$

$$\left(\frac{\partial}{\partial t} + \bar{u} \frac{\partial}{\partial x} - Pr^{-1} Re^{-1} \nabla^2 \right) T' + \frac{d\bar{T}}{dz} w' = 0 \quad (2.2)$$

where

$$\nabla_{H^2}^2 = \frac{\partial^2}{\partial x^2} + \frac{\partial^2}{\partial y^2}, \quad \nabla^2 = \nabla_{H^2}^2 + \frac{\partial^2}{\partial z^2}$$

and \bar{u} is the basic flow, \bar{T} the basic temperature, w' the vertical component of the perturbation velocity, and T' the perturbation temperature. All quantities in (2.1) and (2.2) are dimensionless. The horizontal components of the perturbation velocity u' and v' are derived from the following equations:

$$\left(\frac{\partial}{\partial t} + \bar{u} \frac{\partial}{\partial x} - Re^{-1} \nabla^2 \right) \zeta' - \frac{d\bar{u}}{dz} \frac{\partial w'}{\partial y} = 0 \quad (2.3)$$

$$\nabla_{H^2}^2 u' = - \frac{\partial \zeta'}{\partial y} - \frac{\partial^2 w'}{\partial x \partial z} \quad (2.4)$$

$$\nabla_{H^2}^2 v' = \frac{\partial \zeta'}{\partial x} - \frac{\partial^2 w'}{\partial y \partial z} \quad (2.5)$$

where $\zeta' = \frac{\partial v'}{\partial x} - \frac{\partial u'}{\partial y}$, the vertical component of vorticity.

We now assume perturbations of the form

$$\begin{pmatrix} u' \\ v' \\ w' \\ \zeta' \\ T' \end{pmatrix} = \begin{pmatrix} U \\ V \\ W \\ Z \\ \Theta \end{pmatrix} \exp \{ i(k_x x + k_y y) + \sigma t \} \quad (2.6)$$

where k_x and k_y are the wavenumbers in the x and y directions, respectively, and U, V, W, Z , and Θ are the respective complex amplitude functions. Frequency σ is generally complex and is expressed by $\sigma = \sigma_r + i\sigma_i$ in which a positive value of σ_r denotes the amplification rate of an unstable perturbation. Substituting (2.6) into (2.1) to (2.5), we obtain

$$\begin{aligned} \left[\left\{ \sigma + ik_x \bar{u} - Re^{-1} \left(\frac{d^2}{dz^2} - k^2 \right) \right\} \left(\frac{d^2}{dz^2} - k^2 \right) \right. \\ \left. - ik_x \frac{d^2 \bar{u}}{dz^2} \right] W + Ri k^2 \Theta = 0 \end{aligned} \quad (2.7)$$

$$\left\{ \sigma + ik_x \bar{u} - P_r^{-1} R_e^{-1} \left(\frac{d^2}{dz^2} - k^2 \right) \right\} \Theta - W = 0 \quad (2.8)$$

$$\left\{ \sigma + ik_x \bar{u} - R_e^{-1} \left(\frac{d^2}{dz^2} - k^2 \right) \right\} Z - ik_y \frac{d\bar{u}}{dz} W = 0 \quad (2.9)$$

$$k^2 U = ik_y Z + ik_x \frac{dW}{dz} \quad (2.10)$$

$$k^2 V = -ik_x Z + ik_y \frac{dW}{dz} \quad (2.11)$$

where $k^2 = k_x^2 + k_y^2$. Since a constant temperature lapse rate was assumed, $-d\bar{T}/dz$ was taken to be unity in (2.8).

We assume that both the upper and lower boundary planes are fixed and smooth and maintain constant temperature, i.e.,

$$\left. \begin{aligned} W = \frac{d^2 W}{dz^2} = \frac{dZ}{dz} = 0 \\ \Theta = 0 \end{aligned} \right\} \text{at } z=0 \text{ and } 1 \quad (2.12)$$

Equations (2.7) to (2.11) and the boundary conditions (2.12) are transformed to a set of algebraic equations by approximating the derivatives of the variables with respect to z by finite differences. First, a frequency equation is derived from the finite difference versions of (2.7) and (2.8) subject to the condition of a nonzero value for W and Θ . Then Z can be obtained by solving (2.9) and U and V can be determined from (2.10) and (2.11). The numerical method for solving (2.7) to (2.11) under the boundary conditions (2.12) is the same as that employed in the previous paper (Asai 1970). The numerical calculations in the present paper were performed by making use of a 20-layer representation which was able to provide accurate enough solutions to investigate stability properties of perturbations of the inertial as well as the thermal type.

3. Vertical profiles of the basic flow

Since Helmholtz (1868) discussed stability of a plane parallel flow, a number of people have made fundamental studies of hydrodynamic stability of a parallel flow of inviscid, homogeneous and incompressible fluid. It was proved that when an unstable perturbation exists, a vertical profile of the basic flow $\bar{u}(z)$ must have a point of inflection somewhere in the layer (Rayleigh 1880) and this condition is sufficient to produce instability in symmetric velocity profiles of the basic flow (Tollmien 1935). It was also shown that the phase velocity of an unstable perturbation

must lie within the range of velocity of the basic flow (e.g, Howard 1961).

A study of stability of parallel flow has been extended to a heterogeneous fluid by many workers (Kelvin 1871, Taylor 1931, Goldstein 1931, Drazin 1958, Miles 1961 and 1963, Howard 1961 and 1963, etc.). However, their concerns are primarily with stable stratification, and hence the heterogeneity acts as a stabilizing factor. A variable shear flow in unstably stratified fluid will provide a situation in which two different mechanisms of instability may coexist.

Then the following profiles of velocity are chosen as the basic flow to be studied:

$$\bar{u}(z) = \frac{1}{2} \{1 - (2z-1)^2\}^n, \quad n=1, 2, \dots \quad (3.1)$$

The form (3.1) represents profiles of the basic flow symmetric about the midlevel $z=1/2$ which have a maximum value of $1/2$ and vanish both at the top and the bottom. When $n=1$, (3.1) gives a parabolic profile such as a plane Poiseuille flow. As n increases, a jet-like profile having inflection points becomes sharp. Here we do not refer to any mechanism maintaining the basic flow with such a profile. Figure 1 shows the profiles of $n=2$ (a), $n=1$ (b), and a constant shear (c) for comparison. Circles on the profile (a) indicate the inflection points.

4. Stability characteristics of the flows

Stability properties of a variable shear flow in an unstably stratified fluid are compared with those of a constant shear flow. Figures 2(a), (b), and (c) show the amplification rate of an unstable perturbation as functions of the Richardson number R_i and the vectorial horizontal wavenumber k for the cases (a), (b), and (c) illustrated in Fig. 1, respectively. In these cases $R_a=10^4$ and $k_x=k_y$ were assumed. The Prandtl number P_r is assumed to be unity unless specifically stated otherwise. The neutral stability curve labeled zero in each case separates an unstable domain from a stable one. Amplification rates of unstable perturbations are denoted in units of 10^{-1} by solid lines. Dash-dotted lines indicate the maximum amplification rate. The dotted line in Fig. 2(c) separates a longer stationary unstable perturbation traveling at the mean velocity of the basic flow from a shorter transitive one propagating at a velocity different from the former (see Asai 1970). As is seen from Fig. 2, the unstable domain in case (a) may be divided into two portions having

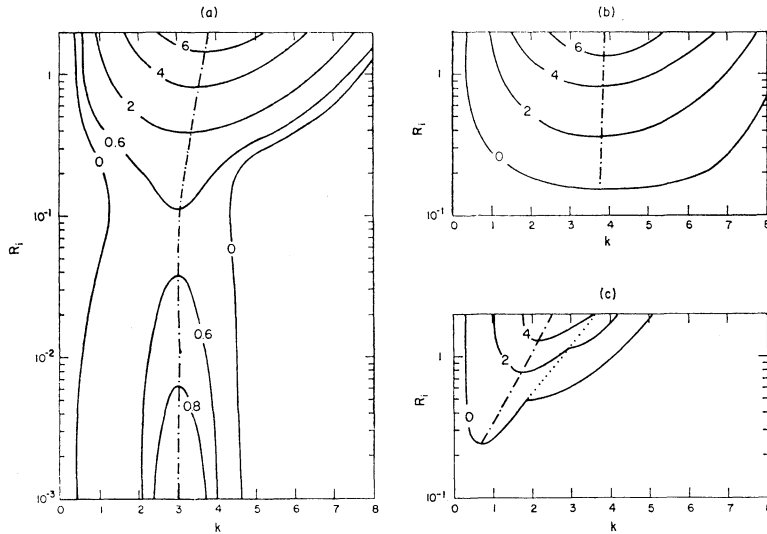


Fig. 2. Stability diagrams for cases (a), (b), and (c). Solid lines indicate the amplification rate in units of 10^{-1} as a function of the Richardson number R_i (ordinate) and the vectorial horizontal wavenumber k (abscissa). The dash-dotted line gives a preferred wavenumber for a given value of R_i . The dotted line in case (c) separates a stationary unstable perturbation from a transitive one. $R_a=10^4$ and $k_x=k_y$ are assumed.

different maximum amplification rates, one for large values of R_i and the other for small values of R_i . Counterparts of the former instability domain are observed in both cases (b) and (c). However, no instability domain corresponding to the latter can be seen in either (b) or (c). It appears that the former is caused by thermal instability modified by a shear flow and the latter is attributed essentially to inertial instability associated with the shear flow having a point of inflection in its velocity profile. For the sake of convenience, the former will hereafter be referred to as thermal instability, while the latter will be called inertial instability.*

Before discussing detailed properties of each unstable perturbation, we will investigate the characteristics of the instability in case (a). Figure 3 shows variation of amplification rate with the Rayleigh number R_a and the Reynolds number R_e for case (a) in which $k_x=k_y=2$ is assumed.

The corresponding Richardson numbers are inserted in the diagram by slanted dashed lines. Amplification rates are shown by solid lines. Again it is seen in Fig. 3 that an unstable domain may be divided into two parts by the dotted line which denotes a minimum amplification rate for a given value of R_a . The borderline between these two parts lies within the range of 10^{-1} to 10^{-2} of R_i for values of R_a ranging from 10^3 to 10^5 . These domains apparently correspond, respectively, to the thermal instability and the inertial instability defined above.

As for the thermal instability, the lowest Rayleigh number at which instability sets in tends to about 700 as the value of R_e decreases. This shows good agreement with the lowest Rayleigh number 712 derived from Rayleigh's (1916) theory of Bénard convection ($R_e=0$) which gives $(\pi^2+k^2)^3/k^2$ as the lowest value of R_a for a given wavenumber k . In the domain of the thermal instability, the amplification rate decreases and the lowest value of R_a increases with increasing R_e . It is evident that the variable shear flow exerts a suppressing influence on the thermal instability and the resulting development of thermal convection regardless of the presence of a point of inflection in the velocity profile of the flow. The other type of instability, i.e., inertial instability, appears when R_e exceeds a critical

* Inertial instability in general implies the instability in which the form of energy transferred between the steady state and the disturbance is kinetic energy. More specifically, here it might be called "inflection-point" instability. However, since no possible confusion is introduced in this paper, the general term "inertial" instability is used to distinguish from the gravitational instability which is referred to as the thermal instability.

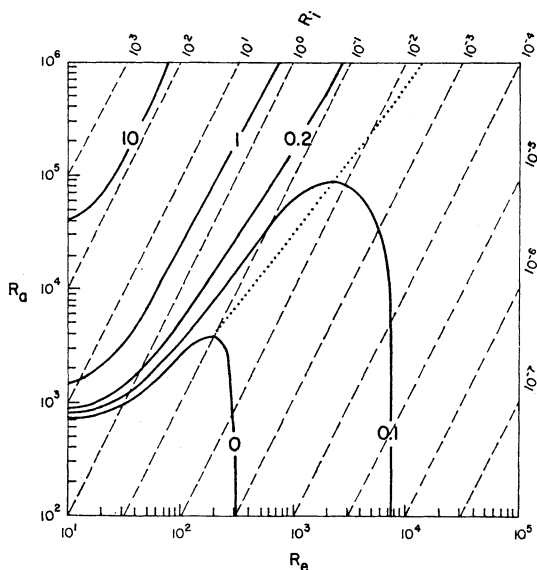


Fig. 3. Stability diagram for case (a) in which $k_x=k_y=2$ are adopted. Solid lines indicate amplification rates against the Rayleigh number R_a and the Reynolds number R_e . Slanting dashed line illustrates the respective Richardson number R_i . Dotted line connecting a minimum amplification rate for a given value of R_a separates the thermal instability domain from the inertial one.

value, about 300 for the present case, in spite of a lower R_a than the critical value, or even a negative value of R_a for which the stratification is stable (not shown here). It is obvious that the instability is not primarily of the thermal type but of the inertial type.

A remarkable difference between the thermal and the inertial instabilities is found in the phase velocity of their perturbations as well. Figure 4 shows variations of the phase velocity in the x direction of the perturbation of $k_x=k_y=2$, $c=-\sigma_i/k_x$, with the value of R_i for $R_a=10^3$, 10^4 , and 10^5 , respectively, shown by solid lines. The variations of amplification rates with R_i are also shown in Fig. 4 by broken lines. As shown in Fig. 4, phase velocities of unstable perturbations change their values very sharply around $R_i=10^{-1}$ which separates the thermal instability from the inertial one. Unstable perturbations of the thermal type travel at a velocity of 0.25 which is nearly equal to the mean velocity of the basic flow averaged over the entire layer (0.27), while unstable perturbations of the inertial type prop-

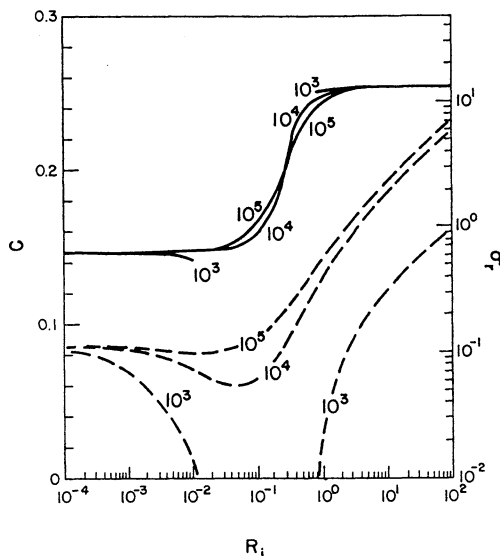


Fig. 4. Variations of phase velocity C (solid lines) and of amplification rate σ_r (broken lines) with the Richardson number R_i for different values of R_a (10^3 , 10^4 , and 10^5). These are for case (a) and $k_x=k_y=2$.

agate at a velocity of 0.15 which is smaller than the velocity of the basic flow at the inflection point in its velocity profile (0.22).

Based on the findings obtained above, we can conclude that a variable shear flow, as well as a constant shear flow, has an inhibiting influence on thermal instability and the resulting development of thermal convection which is imbedded in the flow. Further, for a very small Richardson number another type of instability may appear which is associated essentially with the inertial instability. In addition, it was shown that two different types of instability which may develop in an unstably stratified shear flow can be distinguished from each other in terms of the Richardson number.

5. Unstable perturbations of thermal and inertial types

Now we will examine in more detail the dynamical features of unstable perturbations caused by different mechanisms of instability. In order to clarify the energy conversion processes involved in unstable perturbations as well as their structures, the pertinent energy equation is represented in dimensionless form as follows:

$$\frac{\partial}{\partial t} \langle K' \rangle = \langle P, K' \rangle + \langle \bar{K}, K' \rangle - \langle DK' \rangle \quad (5.1) \quad \text{and}$$

$$\langle P, K' \rangle = R_i \langle F_\theta \rangle e^{2\sigma t} \quad (5.5)$$

$$\langle \bar{K}, K' \rangle = - \langle F_u \frac{d\bar{u}}{dz} \rangle e^{2\sigma t} \quad (5.6)$$

which is derived from the perturbation equation of motion with the aid of the continuity equation and the boundary conditions. The terms in (5.1) are:

$$\langle P, K' \rangle = R_i \langle T' w' \rangle \quad (5.2)$$

$$\langle \bar{K}, K' \rangle = - \langle u' w' \frac{d\bar{u}}{dz} \rangle \quad (5.3)$$

$$\langle DK' \rangle = R_e^{-1} \langle \xi'^2 + \eta'^2 + \zeta'^2 \rangle \quad (5.4)$$

and K' is the kinetic energy of perturbation, \bar{K} is the kinetic energy of the basic flow, P is the potential energy, and they are defined as

$$K' = \frac{1}{2} (u'^2 + v'^2 + w'^2)$$

$$\bar{K} = \frac{1}{2} \bar{u}^2$$

$$P = -R_i z \bar{T}$$

The x , y , and z components of perturbation vorticity are denoted by ξ' , η' , and ζ' , respectively. Angular brackets $\langle \rangle$ denote an average over one wavelength in the x and y directions, respectively, and the entire depth of the layer concerned. As is well known, the first term on the right-hand side of (5.1) represents the conversion of potential energy to the kinetic energy of perturbation, the second term indicates the transformation of the kinetic energy of the basic flow to that of the perturbation, and the last term expresses dissipation due to viscous friction.

By making use of (2.6), (5.2) and (5.3) yield

Here $F_\theta = \frac{1}{2} (\Theta_r W_r + \Theta_i W_i)$ and $F_u = \frac{1}{2} (U_r W_r + U_i W_i)$, and the subscripted variables A_r and A_i denote the real and imaginary parts of A , respectively, where A stands for U , W , and Θ . Then the ratio between the two conversion terms is

$$\frac{\langle \bar{K}, K' \rangle}{\langle P, K' \rangle} = - R_i^{-1} \frac{\langle F_u \frac{d\bar{u}}{dz} \rangle}{\langle F_\theta \rangle} \quad (5.7)$$

First, let us look at the structures of unstable perturbations in case (a). Figure 5 shows the vertical profiles of an unstable perturbation of the thermal type of $R_i=1$ and of the vertical fluxes of heat and momentum due to the perturbation, while Fig. 6 shows those of an unstable perturbation of the inertial type of $R_i=10^{-4}$. Both of them are for $R_a=10^4$ and $k_x=k_y=2$. Amplitudes as well as phase angles of the temperature, the vertical velocity and the x component of velocity are denoted by solid, broken, and dash-dotted lines, respectively. Vertical transport of heat and momentum, F_θ and F_u , are shown by solid and broken lines, respectively. As seen in Fig. 5, the maximum amplitude of temperature, as well as that of vertical velocity, is located at the midlevel, and differences in their phase angles are rather small throughout the depth of the layer. This results in an effective upward transport of heat

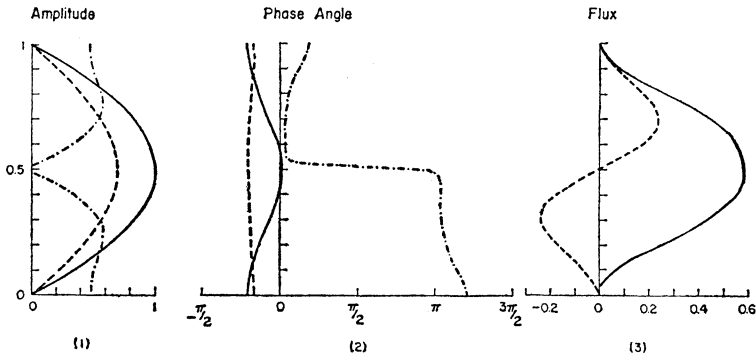


Fig. 5. Vertical structure of an unstable perturbation of the thermal type ($R_i=1$) for case (a): (1) amplitudes normalized so that the maximum amplitude of temperature is unity, (2) phase angles of temperature (solid), vertical velocity (broken), and x component of velocity (dash-dotted), respectively, and (3) vertical fluxes of heat, $2F_\theta$ (solid) and of horizontal momentum u , $2F_u$ (broken). This is for $R_a=10^4$ and $k_x=k_y=2$.

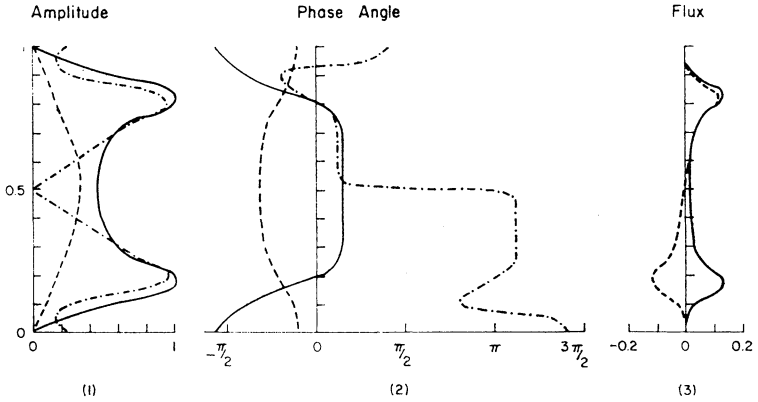


Fig. 6. Vertical structure of an unstable perturbation of the inertial type ($R_i=10^{-4}$). Others are the same as Fig. 5.

as shown in Fig. 5(3). A sharp shift in the phase angle of u at the midlevel is out of phase with w in the lower half layer and in phase with w in the upper half layer so that vertical transport of horizontal momentum results in transforming the kinetic energy of the basic flow to that of the perturbation. Essentially, those characteristics are similar to those of the corresponding stationary unstable perturbation in a constant shear flow.

One of the most remarkable features in Fig. 6 is the temperature profile split into two maximum amplitudes which are located around the points of inflection of the basic flow in the upper and the lower parts of the layer, respectively. Furthermore, except for two thin restricted layers around the points of inflection, phase angles of the temperature differ from those of the vertical velocity by as much as $\pi/2$. This greatly reduces the amount of upward transport of heat as shown in Fig. 6(3). As for the momentum transport, we can observe a feature similar to that in Fig. 5. Energy conversion processes associated with perturbations both of the thermal and the inertial types are compared with each other:

$$\begin{aligned} \langle \bar{K}, K' \rangle &= 0.48 && \text{for the thermal type} \\ \langle \bar{P}, K' \rangle &= 0.12 \times 10^5 && \text{for the inertial type} \end{aligned}$$

There is an indication that the potential energy is a primary source for an unstable perturbation of the thermal type, while the source is completely dominated by the kinetic energy of the basic flow for that of the inertial type.

Examination is extended to perturbations of different geometrical mode because the geometry of perturbations is one of the important factors

in describing characteristics of thermal convection in a shear flow. The variations in the amplification rate of unstable perturbations with the ratio of wavenumber in the y direction to that in the x direction are shown in Fig. 7 for different

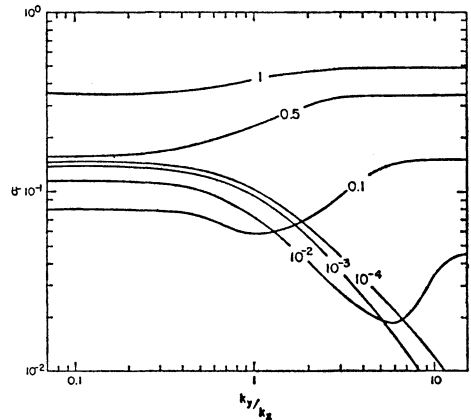


Fig. 7. Variations of amplification rates with the ratio between the wavenumber in the x and y directions k_y/k_x for different values of R_i . Here $R_a=10^4$ and $k=2\sqrt{2}$ are assumed.

values of R_i . These are for case (a), and again $R_a=10^4$ and $k=2\sqrt{2}$ are assumed. The most significant feature in Fig. 7 is the presence of two different types of variation of the amplification rate. One amplification rate is the type which increases with increasing k_y/k_x as observed for larger values of R_i corresponding to perturbations of the thermal type. This feature is the same as that indicated by Asai (1970) for the unstable perturbations in a constant shear flow. However, transverse perturbations still remain

unstable despite a decrease of R_i . Further reduction of the Richardson number beyond a certain value leads to the other type of variation, that is, the amplification rate of a perturbation decreases with an increase in k_y/k_x . Hence it is concluded that a preferred perturbation of the thermal type is of a longitudinal mode, while a transverse perturbation is a preferred mode for unstable perturbations of the inertial type. Thus an unstable perturbation of inertial origin follows Squire's (1933) theorem stating that most unstable wave components in a shear flow are two-dimensional along the flow.

We should note here that some transitional types of amplification rate variation with k_y/k_x appear for intermediate values of R_i , such as 10^{-1} and 10^{-2} in Fig. 7. The amplification rate of unstable perturbations of the inertial type (e.g., $R_i=10^{-2}$) which decreases with increasing k_y/k_x again regains its value for further increase of k_y/k_x when R_a is higher than the lowest R_a for the wavenumber, but remains lower than that of the pure transverse mode.

6. Effect of variable shear on thermal convection

Finally, our attention is focused on the influence of variable shear of the basic flow on perturbations of thermal origin which may be of primary importance for thermal convection. Figure 8 shows variations of amplification rate and phase velocity relative to the mean basic flow with the horizontal wavenumber of a perturbation by solid and broken lines, respectively, for different profiles of the velocity of the basic flow, i.e., cases (a), (b), and (c). Here $k_x=k_y$ is assumed. Variations of amplification rate and energy conversion ratio $\langle \bar{K}, K' \rangle / \langle P, K' \rangle$ with the wavenumber ratio k_y/k_x are shown by solid and broken lines, respectively, for the case of $k=2$ in Fig. 9. Both Figs. 8 and 9 are for the case of $R_a=10^4$ and $R_i=1$ which yields unstable perturbations of the thermal type.

As seen in Fig. 8, an unstable perturbation in the constant shear flow (c) reduces its amplification rate more than that in a variable shear flow, and the reduction is much more striking for perturbations of shorter wavelength in case (c) when the other conditions are the same. Phase velocities of unstable perturbations in cases (a) and (b) increase with increasing wavenumber within the range of velocity of the basic flow. No distinct separation of a longer stationary unstable perturbation traveling at the velocity of

the mean basic flow from the sets of two short transitive unstable perturbations present in case (c) is observed in cases (a) and (b). It is certain

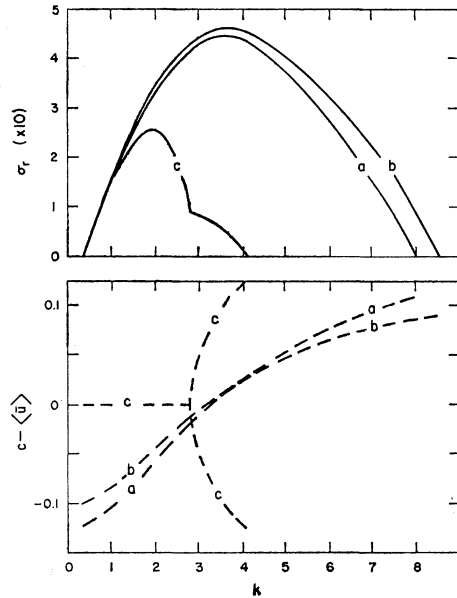


Fig. 8. Amplification rate σ_r (solid line) and phase velocity relative to the respective mean basic flow $C-\langle \bar{u} \rangle$ (broken line) as a function of horizontal wavenumber for different velocity profiles of the basic flow, i.e., cases (a), (b), and (c). Here $R_a=10^4$, $R_i=1$, and $k_x=k_y$ are assumed.

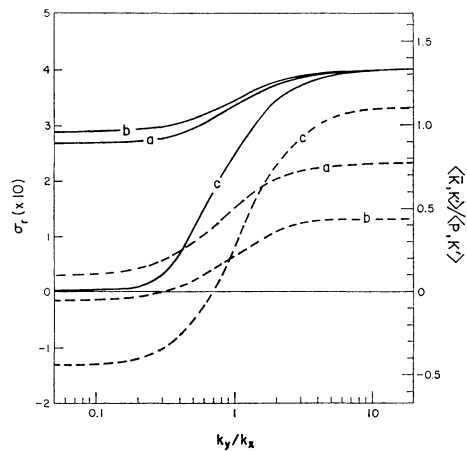


Fig. 9. Variations of the amplification rate σ_r (solid line) and of the energy conversion ratio $\langle \bar{K}, K' \rangle / \langle P, K' \rangle$ (broken line) with the wavenumber ratio k_y/k_x for different velocity profiles of the basic flow and for $k=2$. Others are the same as Fig. 8.

in every case, however, that a most unstable perturbation travels at the velocity of the basic flow averaged over the entire depth of the layer.

Figure 9 shows that a shear flow plays an inhibitive role on a transverse perturbation of the thermal type, and the stabilizing effect is conspicuous for the constant shear flow among the three cases. It is also observed in Fig. 9, as well as in Fig. 8, that there is little difference between (a) and (b). The preference for longitudinal perturbations of the thermal type is primarily affected by a constant shear flow. Conversion of kinetic energy of the basic flow to that of the perturbation in longitudinal modes reverses in transverse perturbations for case (b) as well as case (c). However, no transition takes place for case (a).

7. Conclusions

An investigation was made of stability properties of a vertically variable shear flow in an unstably stratified fluid layer. A system of perturbation equations under the Boussinesq approximation was solved numerically employing a finite difference approximation technique. A primary concern of this study is to clarify the possible influence of a variable shear flow on a thermal convection which is imbedded in the flow. The results obtained in the preceding sections are summarized as follows:

1. Unstable perturbations of two different mechanisms may exist, each of which can be distinguished rather distinctly from the other in terms of the Richardson number. The critical value of the Richardson number lies within the range of 10^{-1} to 10^{-2} . One instability, occurring with larger values of R_i , is of the thermal type which leads to thermal convection modified by the shear flow. The other is of the inertial type (for smaller values of R_i) which is related to the property of the velocity profile of the basic flow.

2. A variable shear flow exerts an inhibiting influence on the thermal instability of transverse perturbations, as does a constant shear flow. The suppressing influence of a variable shear flow on thermal convection is weaker than that of a constant shear flow when the same Richardson number is taken for both cases.

3. A three-dimensional longitudinal mode is most favorable for development of perturbations of the thermal type. On the other hand, an instability of the inertial type is most effective for

two-dimensional transverse perturbations along a vertical plane parallel to the basic flow following Squire's theorem.

Some additional examinations for sharper jet-like velocity profiles [$n > 2$ in (3.1)] and for antisymmetric velocity profiles, such as hyperbolic tangent distribution, seem to require no revision of the main conclusion described here.

8. Remarks

In the present study we adopt smooth boundary conditions at both the upper and the lower boundaries, $d^2W/dz^2=0$. If the rigid boundary condition $dW/dz=0$ is used instead of the smooth boundary condition, another different type of instability may be observed in cases (a) and (b). This is a kind of boundary layer instability, the so-called Tollmien-Schlichting instability, generated close to the boundary. The stability of parallel flow of viscous fluid has been studied by Heisenberg (1924), Tollmien (1929), Schlichting (1933), Lin (1945), and others in conjunction with the stability of a Poiseuille flow and a laminar boundary layer flow. It is then shown that a viscous parallel flow may be unstable in spite of no inflection point in its velocity profile for a certain range of Reynolds number. Stability of stratified plane Poiseuille flow was discussed by Gage and Reid (1967). Much finer grids will be required for representing Tollmien-Schlichting instability when the present numerical method of finite differencing is employed. This aspect will be discussed in a separate paper.

Acknowledgments

The author wishes to thank Drs. A. Kasahara and J.W. Deardorff for their comments on the original manuscript of his paper. Thanks are also due to Mr. G. Browning who assisted in programming part of the computations in this study. The numerical computations were made with the use of a Control Data 6600 computer at NCAR where the author is visiting.

References

- Asai, T., 1964: Cumulus convection in the atmosphere with vertical wind shear: Numerical experiment. *J. meteor. Soc. Japan*, **42**, 245-259.
- , 1970: Three-dimensional features of thermal convection in a plane Couette flow. *J. meteor. Soc. Japan*, **48**, 18-29.
- Chandra, K., 1938: Stability of fluids heated from below. *Proc. Roy. Soc., A*, **164**, 231-242.

- Deardorff, J.W., 1963: On the stability of viscous plane Couette flow. *J. Fluid Mech.*, **15**, 623-631.
- , 1965: Gravitational instability between horizontal plates with shear. *Phys. Fluids*, **8**, 1027-1030.
- Drazin, P.G., 1958: The stability of a shear layer in an unbounded heterogeneous inviscid fluid. *J. Fluid Mech.*, **4**, 214-224.
- Gage, K.S., and W.H. Reid, 1968: The stability of thermally stratified plane Poiseuille flow. *J. Fluid Mech.*, **33**, 21-32.
- Gallagher, A.P. and A. McD. Mercer, 1965: On the behaviour of small disturbances in plane Couette flow with a temperature gradient. *Proc. Roy. Soc.*, **A. 286**, 117-128.
- Goldstein, S., 1931: On the stability of superposed streams of fluids of different densities. *Proc. Roy. Soc.*, **A. 132**, 524-547.
- Graham, A., 1934: Shear patterns in an unstable layer of air. *Phil. Trans. Roy. Soc.*, **232**, **A. 714**, 285-296.
- Heisenberg, W., 1924: Über Stabilität und Turbulenz von Flüssigkeitsströmen. *Ann. Phys.*, **Lpz.**, (4), **74**, 577-627.
- Helmholtz, H., 1868: Über diskontinuierliche Flüssigkeitsbewegungen. Monats. königl. preuss. Akad. Wiss. Berlin, 215-228.
- Howard, L.N., 1961: Note on a paper of John W. Miles. *J. Fluid Mech.*, **10**, 509-512.
- , 1963: Neutral curves and stability boundaries in stratified flow. *J. Fluid Mech.*, **16**, 333-342.
- Ingersoll, A.P., 1966: Convective instabilities in plane Couette flow. *Phys. Fluids*, **9**, 682-689.
- Kelvin, W., 1871: The influence of wind on waves in water supposed frictionless. *Phil. Mag.* (4), **42**, 368-374.
- Kuettner, J., 1959: The band structure of the atmosphere. *Tellus.*, **11**, 267-294.
- , 1967: Cloudstreets. *Aero Revue*, **42**, 52-56 and 109-112.
- Kuo, H.L., 1963: Perturbations of plane Couette flow in stratified fluid and origin of cloud streets. *Phys. Fluids*, **6**, 195-211.
- Lin, C.C., 1945: On the stability of two-dimensional parallel flows, Parts I. II. III. *Quart. Appl. Math.*, **3**, 117-142, 218-234, 277-301.
- Miles, J.W., 1961: On the stability of heterogeneous shear flows. *J. Fluid Mech.*, **10**, 496-508.
- , 1963: On the stability of heterogeneous shear flows, Part 2. *J. Fluid Mech.*, **16**, 209-227.
- Rayleigh, L., 1880: On the stability, or instability, of certain fluid motions. *Scientific Papers*, **1**, 474-487.
- , 1916: On convective currents in a horizontal layer of fluid when the higher temperature is on the under side. *Phil. Mag.*, **32**, 529-546.
- Riis, E., 1962: The stability of Couette-flow in non-stratified and stratified viscous fluids. *Geophys. Publ.*, **23**, 1-37.
- Schlichting, M., 1933: Zur Entstehung der Turbulenz bei der Plattenströmung. Nachr. Ges. Wiss. Göttingen, *Math. Phys. Klasse*, 181-208.
- Squire, H.B., 1933: On the stability of the three-dimensional disturbances of viscous flow between parallel walls. *Proc. Roy. Soc.*, **A. 142**, 621-628.
- Taylor, G.I., 1931: Effect of variation in density on the stability of superposed streams of fluid. *Proc. Roy. Soc.*, **A. 132**, 499-523.
- Terada, T., 1928: Some experiments on periodic columnar formation of vortices caused by convection. *Report Aeron. Res. Inst. Tokyo*, **3**, 1-46.
- Tollmien, W., 1929: Über die Entstehung der Turbulenz. 1. Mitteilung, Nachr. Wiss. Göttingen, *Math. Phys. Klasse*, 21-44.
- , 1935: Ein allgemeines Kriterium der Instabilität laminarer Geschwindigkeitsverteilungen. Nachr. Ges. Wiss. Göttingen., *Math. Phys. Klasse*, **50**, 79-114.

鉛直シャーが高さと共に変り不安定な成層をもつ平面平行流の安定性

浅井 富雄

米国大気科学研究センター

静力学的に不安定な成層をもつ平面平行流が高さと共にその鉛直シャーを変える場合の安定性を摂動論にもとづいて調べ、前に著者(1970)が示した一定シャーに対する結果と比較する。速度プロフィールに曲率のある基本流では性質の異なる2つの型の不安定の発現することがあり、それらは Richardson 数を用いて互いに区別される、一つはシャーの影響を受けた基本的に熱的不安定の型であり、他の一つは成層の影響を受けた慣性不安定のものであって基本流の速度の鉛直プロフィールが変曲点を持つ場合に現われ得る。前者では基本流に平行な方向に波長の長い longitudinal な3次元擾乱が preferred モードとなり、後者では基本流に直角な方向に波長の長い transverse な擾乱が preferred モードとなる。

ここで特に興味のある熱的不安定の擾乱についてみると、シャーのある基本流はその速度プロフィールの変曲点の有無にかかわらず擾乱の発達を抑制し、その抑制作用は transverse モードに対して顕著になる。従って、曲率のあるプロフィールを持つ基本流の熱対流におよぼす影響は一定シャーの場合とほとんど変わらず、また longitudinal な対流 roll の発生にはシャーが基本的な役割を果していることがわかる。Kuettner (1959)の主張する曲率が最も重要という説は支持されない。